Clinal and allometric variation in the skull of sexually dimorphic opossums

Jamile de Moura Bubadué[1,3,4]*, Carlo Meloro[2], Carla Deonisia Hendges[1,3,5], Thaís Flores Battistella[1,3], Renan dos Santos Carvalho[3], Nilton Carlos Cáceres[3]

[1]Programa de Pós-Graduação em Biodiversidade Animal, CCNE, Universidade Federal de Santa Maria, 97105-900, Santa Maria, RS, Brazil.

[2]Research Centre in Evolutionary Anthropology and Palaeoecology, School of Natural Sciences and Psychology, Liverpool John Moores University, 3 Byrom St, Liverpool L3 3AF, United Kingdom.

[3]Laboratório de Mastozoologia, Departamento de Ecologia e Evolução, CCNE, Universidade Federal de Santa Maria, 97105-900, Santa Maria, RS, Brazil.

[4]Laboratório de Ciências Ambientais, Universidade Estadual do Norte Fluminense, 28013-602, Campos dos Goytacazes, RJ, Brazil.

[5]Instituto Federal Farroupilha, Campus Panambi, Rua Erechim, 860, Bairro Planalto, Panambi, Brazil.

*Corresponding author: jamilebubadue@gmail.com, +5555981159348

ORCID: JMB (0000-0001-7069-996X), CDH (0000-0003-3067-3022), TFB (0000-0003-2076-772X), CM (0000-0003-0175-1706), NCC (0000-0003-4904-0604).

Acknowledgements

We would like to thank Diego Astúa, Eliécer Gutiérrez, Geruza Melo, and Cristian Dambros for reviewing this manuscript prior to submission. We are grateful to curators and staff of the MCNFZB (M.M. de A. Jardim), MN (J.A. de Oliveira and S.M. Vaz), MPEG (S.M. Aguiar and J.S. Silva Jr.), MHNCI (V. Abilhoa and S.C. Pereira), UFSC (M.E. Graipel), MACN (D.A. Flores and S. Lucero), and MZUSP (M. De Vivo and J.G. Barros) for granting access to specimens and providing support during our visits to their institutions. This study was financed in part by the Coordenação de Aperfeiçoamento de Pessoal de Nível Superior – Brasil (CAPES) – Finance Code 001 for JMB, CDH and TFB. JMB was also supported by CAPES 194 sandwich PhD program/Process number 88881.189949/2018-01. CM was supported by the British Research Council under the Research Links program (Grant No. 127432108). NCC has a research fellowship in Ecology, granted by the Conselho Nacional de Desenvolvimento Científico e Tecnológico (CNPq), Brazil.

Abstract

Three species of sexually-dimorphic opossums are broadly distributed across South America: the habitat generalist *Didelphis albiventris*, the Atlantic forest-dweller *D. aurita*, and the Amazonian forest-dweller *D. marsupialis*. We used 2D geometric morphometrics to quantify skull size and shape variation in the three opossum species and test the hypothesis that degrees of sexual dimorphism and morphological variation should follow a cline across different South American environments. We first detected a strong impact of allometry on skull shape variation especially in males of the three species that tend to show stronger bite force, which is thought to be related to sexual selection. The degree of sexual dimorphism varies in relation to environmental seasonality. The skull of the plastic species *D. albiventris* showed the strongest ecogeographical pattern, showing conformity to Bergmann's rule in skull size. In this species, size increase and shape changes are associated with colder climates and stronger bite force. Skulls of *Didelphis marsupialis* are moderately impacted by climate, following productivity patterns of tropical regions associated with fruit availability. The most territorial species, *D. aurita*, has the strongest allometric effect and shows no clinal variation. Our results also support a degree of evolutionary constraint on the skull morphology of the three South American opossums. The black-eared opossums clade exhibits a weak (*D. marsupialis*) or nonexistent (*D. aurita*) association between skull morphology and climate. Skull shape changes of *D. aurita* are allometrically driven while those of the white-eared opossums clade (*D. albiventris*) varies in relation to the environment.

Key-words: allometric slopes, biological constraint, Didelphidae, ecomorphology, evolutionary trends, macroecology, Neotropics.

Introduction

The mammalian skull varies considerably between and within clades in relation to a multitude of factors. These includes intrinsic factors such as developmental and biomechanical constraints (Cardini and Polly 2013; Koyabu et al. 2014), as well as extrinsic ones (i.e., environmental variation; Caumul and Polly 2005). In recent years, geographical patterns of mammalian skull variation have received a strong focus especially after the advancements in geometric morphometrics and spatial analyses (dos Reis et al. 2002; Monteiro et al., 2003; Cardini et al. 2007; Adams et al. 2013; Stumpp et al. 2018). More in particular, the study of South American Neotropical clades has revealed strong intra- and interspecific variation related to the environment for several mammalian taxa including primates (Cáceres et al. 2014; Meloro et al. 2014a, b), carnivorans (Bubadué et al. 2016; Schiaffini 2016; Schiaffini et al. 2019), ungulates (Hendges et al. 2016), xenarthrans (Magnus et al. 2018a), rodents, lagomorphs (Maestri et al. 2016; Magnus et al. 2018b), and marsupials (Damasceno and Astúa 2016; Magnus et al. 2017). The high climatic variation registered from the equator to the southern part of South America had a significant impact on mammalian skull variation and diversification at all taxonomic and ecological levels. Nevertheless, intrinsic factors related to species biological characteristics (i.e., sexual dimorphism, biomechanical performance) still showed a strong association with skull shape variation of South American mammals (Astúa 2010; Hendges et al., 2019). Within sexually dimorphic species, each sex can be impacted by the environment at different strength, resulting for example in a pattern of sexual dimorphism related to climate (Kelley 1988).

Here, we used three sexually dimorphic marsupials from the genus *Didelphis* as biological models to assess the relative influence of intrinsic and extrinsic factors on skull size and shape variation: the Brazilian white-eared opossum *D. albiventris,* a habitat generalist widely distributed in South America occurring mainly in savannahs and grasslands; the southern black-eared opossum *D. aurita*, a forest dweller restricted to the Atlantic forest; and the northern black-eared opossum *D. marsupialis*, a forest dweller whose main occurrence in South America is in the Amazonian forest. Therefore, using a combination of geometric morphometrics (Zelditch et al. 2012) and spatial autocorrelation methods (Diniz-Filho et al. 2003), we aim to characterize opossum's skull size and shape variation at continental scale by testing how sex, allometry, and environmental factors affect skull morphological changes within each species.

We also tested the impact of the environment on sexual size and shape dimorphism (SSD and SShD). When sexual dimorphism is male-biased, Rensch's rule predicts that sexual dimorphism increases with body size (Rensch 1950). Astúa (2010) already identified sexual dimorphism in the skull shape of six *Didelphis* species, including the three species used in this study; however, his work did not explore intraspecific variation of SSD in relation to geography. Post et al. (1999) reported environmental influence in sexual dimorphism patterns demonstrating that warm and stable climates favor the increase of sexual size dimorphism in the red deer (*Cervus elaphus*). Thus, we expect that sexual dimorphism in *Didelphis* will increase in climatically more stable environments as well.

Bergmann's rule predicts that endothermic animals tend to be larger at high latitudes in order to control heat lost better in colder environments (Bergmann 1847). However, the converse of Bergmann's rule trend is often found in small mammals (Belk and Houston 2002;

Medina et al. 2007; Gohli and Voje 2016; Maestri et al. 2016), including other didelphid marsupials such as *Chironectes minimus* (Damasceno and Astúa 2016) and *Caluromys philander* and *C. lanatus* (Magnus et al. 2017). Thus, on size variation of *Didelphis* spp. related to the environment, we expect to find the converse of Bergmann's rule for the three opossum species. We predict that the more generalist species should be more adaptable to environmental changes, meaning that morphological variation in *D. albiventris* related to climate should be stronger than in the smaller specialist, forest-dweller *D. aurita* (Colles et al. 2009).

Materials and Methods

We photographed 413 skulls of *Didelphis*: 197 females from 114 localities and 216 males from 113 localities (for information on each species see Table 1). These samples covered all geographic distribution of *D. albiventris* and *D. aurita*, and the Brazilian Amazon portion of *D. marsupialis* distribution range (see Supplementary Data SD1, Fig. 1). Cardini (2014) demonstrated that the ventral view of the skull is ideal for studies employing 2D data as the results better resemble those of 3D datasets, while dorsal and lateral views provide unusual patterns of shape variation, which poorly match the 3D datasets. Therefore, we positioned the skull of each specimen in ventral view at a fixed distance (1.5 m), aligning on the same optical plane the palate with the camera lens and adding a scale bar at the same height as the palate.

The digital images were landmarked by one of us (TFB) using tpsDig2 ver. 2.26 (Rohlf 2015). We used a total of 25 landmarks, as in Cáceres et al. (2016), to describe features such as the general skull shape, the occipital condyle, the zygomatic arch areas, as

well as the relative size and positioning of the teeth, especially the canine and molars, which were marked individually (Fig. 2). Because the skull is a structure with bilateral symmetry, we accounted for both sides of the skull in the landmark configuration and used the symmetric component of the Procrustes coordinates in all statistical procedures (Cardini et al. 2016).

We performed Generalized Procrustes Analysis (GPA, Rohlf and Slice 1990) to remove differences in size, orientation, and positioning from our original landmark coordinates. This procedure transformed raw landmark coordinates into shape variables (= Procrustes coordinates). Skull size was directly extrapolated from the raw landmark coordinates as the centroid size, that is, the square root of the sum of squared distances of each landmark from the barycenter of each configuration. To prevent pseudoreplication (Hurlbert 1984) and minimize the geographical bias in our data, we used the average values of the Procrustes coordinates and centroid size per locality and sex in all the statistical analyses. Averaged centroid sizes were transformed in natural logarithm to properly scale them relative to the mean (Dryden and Mardia 1998; Meloro et al. 2008; Cáceres et al. 2014; Meloro et al. 2014a, b).

In order to study the geographical patterns of sexual size (= SSD) and shape (= SShD) dimorphism, we subdivided our sampled geographical locations with a grid and then computed mean male and female skull size to calculate SSD (= difference between male and female mean sizes) per species per each cell of the grid. For shape, we averaged the male and female Procrustes coordinates and calculated the Procrustes distance between them in each grid to generate the SShD values. We used a grid with a 1.5 x 1.5 degrees cell resolution in order to maximize the number of useful cells as to have at least one individual

of both sexes for each species in a cell. Grids were placed separately for each species. The original dataset reduced localities to 50 useful cells following the criteria explained above (Table 1, Supplementary Data SD2).

We used a Principal Components Analysis of the symmetric shape component to visualize variation between species and sexes in MorphoJ (Klingenberg 2011). Two-way Procrustes ANOVA was performed to test for differences between species and sexes in both size and shape using the R package 'geomorph' (Adams et al. 2018). We tested for differences in the allometric slopes of species and sexes by running a homogeneity slope test (that is, the interaction term between size and species and/or sex) with the function procd.lm. We ran 9,999 permutations to validate reliability of the P value. Additionally, following Piras et al. (2011) and Sansalone et al. (2015, 2018) we also tested for different degrees of shape differences at specific standardized size values. This is accomplished by adding residuals shape coordinates to the expected [by allometric equation] corresponding shapes at the size chosen (Zelditch 2012). The function 'lm.rrpp' associated with 'pairwise', both from package 'RRPP'(Collyer and Adams 2018), were employed to test for species and sexes pairwise shape differences, using the distances between means method, for each group pairs in this new set of "standardized by specific size value" shape coordinates. This procedure was done for comparisons of shape at large and small comparable sizes (Piras et al. 2011).

For each specimen, we recorded the geographic coordinates of its collection locality (see Supplementary Data SD1; Fig. 1), using DIVA-GIS 7.5 software (http://www.divagis.org/download), and extracted 19 bioclimatic variables with 2.5 arc-minutes resolution from the WorldClim raster database (Hijmans et al. 2005). We performed a PCA analysis of the 19 bioclimatic variables and selected only the first five PCs, which

cumulatively explained 95% of the environmental variance. We used this threshold to keep with the same one generally used for morphological data (Zelditch et al. 2012).

Because our data are geographically distributed, spatial autocorrelation must be accounted for (Diniz-Filho et al. 2003). We performed an Eigenvector-based spatial filtering to generate the spatial filters to be included in our final models. This procedure was performed with the R package 'vegan 2.0' (Oksanen et al. 2012) by running a Principal Coordinates of Neighbor Matrices (PCNM) (Dray et al. 2006; Borcard et al. 2011) to create independent spatial variables that represent the spatial relationship among our skulls sampling-site. We obtained the PCNM variables from the Principal Coordinate Analysis (PCA) of the truncated geographic distance matrix between sampling sites (Dray et al. 2006). This procedure and the bioclimatic variables PCA were made each time we performed the tests with the different subsamples (genus level, sexual dimorphism grids, and species level).

We employed variation partitioning based on redundancy analysis (RDA) (Dray et al. 2006; Borcard et al. 2011) to evaluate the singular contribution to skull size and size-free shape variation of four distinct factors: species; sex; climate, described by the selected climatic PCs; and geography, described by the selected PCNM. Size-free shape coordinates were extracted as residuals of allometric regressions. They were employed at the genus level analyses only because variation partitioning allows four predictors at a time. We did the same procedure for SSD and SShD to test the impact of three exploratory factors: species, climate, and geography. The PC scores of shape variables that cumulatively explained 95% of the total shape variance were used as response variables in the variation partitioning models (Zelditch et al. 2012). Before running each variation partitioning model, we used a covariance matrix to select only the PCs of climate and PCNM variables that were significantly

correlated with skull shape and size (selected variables detailed at the supplementary materials). In the case of *D. aurita*, no climatic PC was significantly correlated to skull size, and so we only ran the analysis with two components: sex and geography. We used adjusted R^2 values to assess the contribution of each predictor while controlling for the others, and the fraction of interaction between them (Borcard et al. 2011) and computed variation partitioning using the R package 'vegan 2.0' (Oksanen et al. 2012). To visualize the general climatic patterns in the univariate responses (SSD, SShD, and size variance in each species), we plotted the selected PC that holds the highest percentage of variance of climate data as predictor. To visualize the shape data of each species in relation to climate variables, we present Partial Least Squares plots generated in TpsPLS (Rohlf 2015) with associated shape deformations when the model was significant and compared the PLS angle vectors between species using MorphoJ (Klingenberg 2011). This test allowed to detect if climatic skull shape variation follow the same pattern between species (Meloro et al. 2014a, b).

All the data generated and analyzed during this study are included in this published article and its supplementary data files.

Results

PCA of shape variables showed extensive overlap between species and sexes, especially between *D. aurita* and *D. marsupialis*. The first PC explained 57.23% of shape variance and showed some degree of separation between males and females, with males occupying the most positive scores of PC1 and females the most negative ones (Fig. 3). At the positive end of PC1, deformation plots showed proportional shortening and thinning of the muzzle area, smaller occipital condyle and foramen magnum, molars, and incisors, and

the increase of the zygomatic arch relative length and canines while the opposite occurred on negative scores (Fig. 3). PC2 explained 15.18% of shape variance and separated *D. albiventris* specimens at the positive scores, from the other two species, at negative scores (Fig. 3). At the positive end of PC2, the skull tends to be shorter and thicker. Molar teeth are proportionally larger, while canines are smaller and the zygomatic arch is thicker, but shorter in length (Fig. 3). Still, species and sexes explained a significant proportion of skull shape (species: $R^2 = 0.107$, $F = 16.303$, $P < 0.001$; Sex: $R^2 = 0.162$, $F = 49.516$, $P < 0.001$) and size (species: $R^2 = 0.448$, $F = 107.252$, $P < 0.001$; sex: $R^2 = 0.088$, $F = 42.239$, $P < 0.001$) variations. No interaction between species and sex could be found on shape ($R^2 = 0.007$, $F = 1.062$, $P = 0.171$) and size ($R^2 = 0.001$, $F = 0.282$, $P = 0.548$).

Size explained a considerable amount of skull shape variation in the total sample ($N = 227$, $R^2 = 0.148$; $F = 39.010$, $P < 0.001$). The allometric slopes between species and sexes were significantly different (Group allometries: $R^2 = 0.047$, $F = 2.989$, $P < 0.001$; Fig. 4). *Didelphis albiventris* and *D. marsupialis* samples for both sexes and *D. aurita* females had different slope lengths from that of *D. aurita* males (Table 2). Regarding the angle between slopes, *D. albiventris* (both sexes) differs from *D. aurita* males and *D. marsupialis* (both sexes). Males of *D. albiventris* also differ from both sexes of *D. marsupialis* (Table 2). Allometric convergence test confirmed this, showing significant shape differences at all large size comparisons and in the following pairs at small sizes: *D. albiventris* females-D. *aurita* (both sexes), *D. albiventris* (both sexes)-*D. marsupialis* females, *D. albiventris* males-*D. aurita* females, *D. aurita* females-*D. aurita* males, *D. aurita* females-*D.* marsupialis males, and *D. aurita* males-*D. marsupialis* females (Table 3).

Regression models performed independently for each taxon demonstrate all species and sexes to be impacted by allometry at different strengths (*D. aurita* male 51.39% > *D. albiventris* male 49.59% > *D. albiventris* female 29.69% > *D. aurita* female 24.89% > *D. marsupialis* male 14.81% > *D. marsupialis* female 12.05%, see Fig. 4). In general, the largest specimens tend to have proportionally more elongated zygomatic arches (but not necessarily wider), smaller foramen magnum, larger canines, and relatively smaller molars. In males, the muzzle is evidentially shorter in all species and the zygomatic arch also becomes wider (maximum in *D. aurita* male), but these changes are less apparent in females (Fig. 4).

Within-genus models

Skull morphology

Variation partitioning showed that, as pure components, sex (7%) and species (7%) followed by geography (5%) and climate (1%) are the best predictors of skull size variation (see Fig. 5a and Supplementary Table 1). For skull shape size-free, sex was the most important factor, explaining 14% of variation, followed by species (7%), and the interaction between species, climate, and geography (7%). Geography interaction with species explains 4% of shape variation (Fig. 5b and Supplementary Table 1). The pure components of geography and climate were not significant for skull shape (Supplementary Table 1).

Sexual dimorphism

Didelphis aurita has the highest mean values of SSD (*D. aurita:* 0.080 > *D. albiventris:* 0.078 > *D. marsupialis:* 0.058) and SShD (*D. aurita:* 0.039 > *D. albiventris:* 0.033 > *D.*

marsupialis: 0.027). However, the variation of sexual dimorphism in skull size (SSD) and shape (SShD) recorded across different geographical grids did not differ between species (N = 50, Size: $F_{2,47}$ = 1.408, P = 0.252; Shape: $F_{2,47}$ = 0.259, P = 0.771). Variation partitioning analysis supported this with species as a pure component being not significant for both SSD and SShD. In all cases, climate and geography explained most of the sexual dimorphism variation in skull size and shape (see Fig. 5c, d) with climate vector being generally loaded on seasonality although they are correlated with different climatic principal components (SSD is correlated to PC1 while SShD is to PC4 of climate, see Supplementary Materials). A plot showing SSD and SShD variation in relation to climate vector shows dimorphism to be higher in more seasonal environments for both size and shape and that SSD is negatively correlated with temperature, while SShD is positively correlated to temperature range (Fig. 6, Supplementary Materials).

Within-species models

Didelphis albiventris

Variation partition model showed that skull size is primarily explained by the interaction between climate and geography (40%), followed by sex (9%), but the pure components of climate and geography are not significant (see Supplementary Fig. 1a and Supplementary Table 3). PCClimate1 correlates positively with annual mean temperature and mean temperature of coldest quarter and negatively with temperature seasonality. As size and PCClimate1 had a negative correlation, skull size decreases in warmer and less seasonal environments (Figure 7a).

For skull shape, size was the most important predictor, explaining 24% of variation, followed by the interaction of size, climate, and geography (12%), the interaction between sex and size (11%), and sex as a pure component (4%) (see Supplementary Fig. 2a and Supplementary Table 3). PLS summarizes the relationship between shape and climate. The first block of PLS is positively correlated with PCClimate1 ($r = 0.942$) and holds 96.31% of total variation (PLS1: $r = 0.460$, $P < 0.001$). In positive scores of PLS, where temperatures are high, with low seasonality, *D. albiventris* has proportionally shorter and smaller zygomatic arches, wider muzzle, and smaller canines than specimens with lower PLS scores living in colder and more seasonal areas (Fig. 7c).

Didelphis aurita

Skull size variation in the Atlantic forest black eared opossum was primarily explained by sex (32%), followed by geography (3%), and the interaction between geography and sex (3%) (see Supplementary Fig. 1b and Supplementary Table 4). For skull shape, size was the most important predictor of shape, explaining 34% of variation, followed by the interaction of size and sex (25%). Climate and geography as pure components were significant in the variation partitioning model, but with low percentage of explanation (both 2%) (see Supplementary Fig. 2b and Supplementary Table 4). This is confirmed by PLS that was not significant for *D. aurita* skull shape vs climate (PLS 1 holds 64% of total variation, $R = 0.255$, $P = 0.385$).

Didelphis marsupialis

Skull size was primarily explained by climate interacting with geography (10%), followed by sex (7%) (see Supplementary Fig. 1c and Supplementary Table 5). PCClimate1 of the *D. marsupialis* sample positively correlated with annual mean temperature, mean temperature of coldest quarter, precipitation of coldest quarter and negatively with temperature annual range and mean diurnal range (= mean of monthly (max temp - min temp)). As size and PCClimate1 were positively correlated, size increases in warmer environments that have higher precipitation rates in the winter and have low diurnal and annual temperature range (Fig. 7b).

For skull shape, sex was the most important predictor of shape, explaining 6% of variation, followed by size (4%), climate, size and geography interaction, and geography as a pure component explaining only 3% of shape variation (however, geography as a pure component was not significant; see Supplementary Fig. 2c and Supplementary Table 5). PLS summarizes the relationship between shape and climate. The first block of PLS is negatively correlated with PCClimate4 (R = - 0.943) and holds 60.22% of total variation (PLS1 R = 0.458, P = 0.054). PCClimate4 positively correlates with mean diurnal range and isothermality, and negatively correlates with temperature seasonality (Supplementary Materials). Thus, at positive scores of PLS, *D. marsupialis* has proportionally longer and thinner zygomatic arches and longer and thinner muzzle area in areas where diurnal range and isothermality are lower and temperature seasonality is higher (in positive scores, Fig. 7d).

PLS vector comparisons

As the *D. aurita* PLS was not significant, we only compared the vector directions between *D. albiventris* and *D. marsupialis*. The direction of PLS shape vectors due to climate between these species were not statistically distinct from an angle of 90º (angle = 81.600, P = 0.333), meaning that the patterns of shape change due to climate between these species do not follow parallel directions.

Discussion

Our results reinforce the observation that *Didelphis* species are significantly different in size and shape of the skull and present sexual dimorphism. *Didelphis aurita* and *D. marsupialis* exhibit an extensive overlap in morphospace as both show thinner and longer skulls, in comparison to *D. albiventris*. They are also larger in size than *D. albiventris.* This is congruent with the findings of Astúa (2015) who found less separation between the two forest-dwellers opossum species. Indeed, *D. aurita* and *D. marsupialis* have more similar ecological requirements and are more closely related to each other than to *D. albiventris* (Costa and Patton 2006; Rossi et al. 2012; Dias and Perini 2018). Molecular analyses based on cytochrome B show only 2.8% difference between *D. aurita* and *D. marsupialis*, and *D. albiventris* differs 5.7% from the last clade (Costa and Patton 2006). Regarding sexual dimorphism, male opossums exhibit a shorter muzzle area and larger zygomatic arches and canines than females. This pattern of shape deformation is also detectable in the allometric regressions.

Allometry tends to be stronger in males of *D. aurita* and *D. albiventris* and, in most cases, supports divergent allometric patterns between species and sexes as it increases shape differences between them at large comparable sizes (Piras et al. 2011; Sansalone et

al. 2015, 2018). These two species have larger size variation in our sample than *D. marsupialis*. Previous works concluded that the strong allometric patterns in marsupials are related to the amount of size variation within the group, which can be enforced by the continuous growth of marsupials, even in adulthood (Astúa de Moraes 2000; Astúa 2015). The potential of males to grow in accelerated rates, and therefore having more size variation than females in adulthood supports our hypothesis favoring stronger allometric patterns among them. Skull allometry generally selects traits which enhances bite force (larger temporal muscle area and shorter muzzle, Van Valkenburgh, 1991; Damasceno et al. 2013, Hendges et al. 2019) and the enlargement of the canine tooth width (important for fighting and killing among mammals, Ungar 2010). This can be detected mostly in males of all species, suggesting an intrinsic relationship in these marsupials for an association between bite force and size. This may have been favored by the reproductive behavior of *Didelphis* , where males tend to fight between each other during mating season, seeking for mates, and females present more territoriality, and therefore a strong bite would be advantageous for both sexes, but especially males (Ryser 1992; Cáceres 2003; Cáceres and Machado 2013). Field studies show that aggressiveness when males are captured during breeding season tends to be more intense than during the rest of the year (Cáceres 2003; also observed during field work by the authors JMB and NCC). This was also observed for the congeneric North American species *D. virginiana* (Ryser 1992). Julien-Laferrière and Atramentowicz (1990) stated that the strategy of *D. marsupialis* is to completely stop reproductive activity in periods of food shortage, so that in their breeding seasons resources are always sufficiently available. The enhancement of the allometric slopes in each species could possibly be related to the degree of aggressiveness they present during mating

seasons, explaining why *Didelphis aurita* has the strongest relation between size and shape, with proportionally the largest bite forces, followed by *D. albiventris* and lastly by *D. marsupialis*.

A geographical pattern of skull morphology within the genus was expected as it mirrors mostly the differences among species that occur in different ecoregions, like *D. marsupialis* occurring in the Amazon forest, *D. aurita* in the Atlantic forest and *D. albiventris* occurring mostly in biomes like savannahs and grasslands (Gardner 2007). Variation partitioning confirms this, as most of the climatic variation detected cannot be separated from species and the geographic eigenvectors (the three predictors interaction explains 25% of size and 7% of shape variation, see Fig 5). Interestingly, sexual dimorphism scores do not differ between species, but correlate with climate (9% of SSD and 7% of SShD, Supplementary Fig. 1) and geography (15% of SSD and 11% of SShD, Supplementary Fig. 1). This confirms that sexual dimorphism can be affected by environmental conditions. However, *Didelphis* does not follow the same trend as the red deer, where sexual dimorphism increases towards warm and stable environments (Post et al. 1999). Instead, sexual dimorphism in *Didelphis* increases towards colder (SSD) and more seasonal environments (SSD and SShD). Considering that these animals are territorial (in the case of females) and possess behavioral aggressiveness (especially males), it is possible that this behavior increases in areas where some food type of resources, such as fruits and vertebrate prey, are not available throughout the year (Cáceres 2002, 2003; Ryser 1992; Cáceres and Machado 2013). If this is true, SSD and SShD can be favored by intraspecific competition. Because males have a larger home range than females (Sunquist et al. 1987; Cáceres and Monteiro-Filho 2001), their foraging behavior and diet could also

be sexually discrepant as well (Cáceres 2003; Mendel et al. 2008). We cannot be sure about this because we could not find any study that analyzes sexual differences in opossum diet at different geographical regions, but sexual differences in diet of other mammals was previously found (Birks and Dunstone 1985; Begg et al. 2003; McLean et al. 2005). *Didelphis* spp. are opportunistic feeders and have large diet variation, especially related to seasonality and so we can expect variation in degree of sexual dimorphism in relation to food availability (Julien-Laferrière and Atramentowicz 1990; Cáceres 2002, 2003; Mendel et al. 2008, Ceotto et al. 2009).

Didelphis albiventris follows a clear and strong pattern of Bergmann's rule for size, becoming larger in more seasonal and colder environments. We have expected the opposite, that they would follow the reverse Bergmann's rule, like other small mammals (see Belk and Houston 2002; Medina et al. 2007; Gohli and Voje 2016; Maestri et al. 2016), including the didelphids *Chironectes minimus* (Damasceno and Astúa 2016) and *Caluromys philander* and *C. lanatus* (Magnus et al. 2017)). However, the Bergmann patterns for *D. albiventris* are congruent to trends found in mid-size to larger mammals, like the crab-eating fox *Cerdocyon thous* (Bubadué et al. 2016). Although a placental carnivore, this is an opportunistic species and presents similar distributional range to *D. albiventris*, also occurring in both grassland and forest environments (Gardner 2007; Bubadué et al. 2016). *Didelphis aurita* shows no climatic trend, with size being spatially structured, but the main factor explaining its variation is still sexual dimorphism. *Didelphis marsupialis* also exhibits a climatic trend in size, but it does not follow Bergmann's prediction. In this species, skull size increases in areas with higher temperatures, where diurnal and annual temperature ranges less and where precipitation tends to be higher in the coldest season.

This shows that the morphological variation in *D. marsupialis* can be related to habitat productivity (Meiri et al. 2007), as fruit availability seems to positively correlate with rainfall in tropical regions (Fleming et al. 1987).

Like size, the effect of climate on the skull shape is strong for *D. albiventris*, moderate for *D. marsupialis*, and nonexistent for *D. aurita*. Clinal variation of skull shape in *D. albiventris* is spatially structured and interacts with allometry. Indeed, cranial deformations towards a more seasonal and colder environments are congruent with those of allometry, keeping with our initial hypothesis that allometry selects traits that might help in a less resourceful environment. Food availability tends to vary more often in seasonal areas and diet studies on *Didelphis* have shown great variability of food frequency over the year (Cáceres 2002; Cantor et al. 2010; Silva et al. 2014). Climatic instability in high latitudes can favor the selection of traits that enhance food processing and capturing, facilitating the consumption of harder food items. Indeed, in omnivores, these morphotype shifts (larger zygomatic arch and canines, and smaller snout area) can increase the amplitude of food items that can be consumed and similar pattern were identified in other South American groups (e.g., capuchin and howler monkeys: Cáceres et al. 2014; Meloro et al. 2014a, b; peccaries: Hendges et al. 2016, 2019; and in woolly opossums: Magnus et al. 2017). *Didelphis marsupialis* showed a distinct pattern of clinal variation as supported by PLS vector comparison (angle = 81.600, P = 0.333). Like size, the climatic variables important for shape variation in the forest dweller *D. marsupialis* are distinct from the generalist *D. albiventris. Didelphis marsupialis* enhances molar area, showing thinner and longer muzzle and zygomatic arch in localities with low diurnal range, low isothermality, and high temperature seasonality. This may be possibly due to an increase in fruit intake throughout

the year (Julien-Laferriere and Atramentowicz 1990). Seasonal areas favor selection on skulls characterized by larger molar areas (Cáceres et al. 2014; Meloro et al. 2014a, b; Bubadué et al. 2016; Hendges et al. 2016, 2019). It is possible that also the Amazonian opossum species are more fruit dependent than the other species. In fact, the extinct species from the late Miocene of Amazonia, *D. solimoensis*, like *D. marsupialis*, tended to be even more frugivorous than the living counterparts, such conclusion based on the molar morphology (Cozzuol et al 2006). However, it is important to notice that our samples are only within the Brazilian Amazon and the distributional range of *D. marsupialis* is much wider than that (Gardner 2007).

The phenotypic plasticity of each species – a property of the individual genotype to produce different phenotypes when exposed to different environmental conditions (Pigliucci et al. 2006) – explains the geographical pattern found in our study. Indeed, *D. albiventris* is one of the most generalist and widespread opossum species of South America (Costa and Patton 2006). Generalist species tend to be morphologically more plastic than those narrow-niche species (i.e., specialists) and, when they have a broad geographical range, such as *D. albiventris*, they might produce greater variation among individuals than specialist species, such as *D. aurita* and *D. marsupialis*, because generalist species usually occur in a broad scale of different environments (see Pigliucci et al. 2006; Hendges et al. 2016). Cáceres and Machado (2003) compared *D. albiventris* and *D. aurita* habitat use in the field and concluded that *D. aurita* seems to be more dominant towards the forest domain than *D. albiventris*, where food resources are more abundant during mating season. Astúa (2015) pointed out that the white-eared opossum clade, which includes *D. albiventris,* tends to have a more plastic tendency for morphological changes than the black-eared opossum clade, which includes *D.*

aurita and *D. marsupialis*. This means that shape changes in the skull of the black-eared clade are much more allometric than in the white-eared clade, also due to the fact that the black-eared opossums are more restrict towards their environmental conditions. We expected that morphological trends between *D. aurita* and *D. marsupialis* would be more similar due to their ecological preferences (dense forest) and phylogenetic history, but this does not seem to be the case as *D. aurita* showed no climatic pattern while *D. marsupialis* does. Biogeographical analyses by Dias and Perini (2018) on *Didelphis* suggest an Amazonian origin for the black-eared opossum clade (*D. aurita – D. marsupialis*), which is congruent with the Miocene fossil records from Amazon (Cozzuol et al. 2006). If this is true, this would place the Atlantic forest *D. aurita* as a derived species, supporting the lack of association of their skull morphology with climate, in part due to its smaller geographic range (Fig. 1).

In summary, we found that the three species of *Didelphis* differ in skull size and shape patterns, including allometric trends, but not for sexual dimorphism. Interestingly SSD and SShD vary following geographical and environmental clines suggesting that on regional scale *Didelphis* are morphologically flexible. Skull shape and size clines could also be found in *D. albiventris* and *D. marsupialis* in relation to their wide range and broad ecological niches. *Didelphis aurita* instead shows no ecogeographical variation, possibly due to their smaller distributional range, but it is the species with more allometric effect. This study emphasizes the need of more comparative intrageneric research with other mammalian groups, as species within a genus could respond very differently regarding phenotypic changes.

References

Adams DC, Collyer ML, Kaliontzopoulou A (2018) Geomorph: software for geometric morphometric analyses. R package version 3.0.6. Available at: https://cran.r-project.org/package=geomorph

Adams DC, Rohlf FJ, Slice DE (2013) A field comes of age: geometric morphometrics in the 21st century. Hystrix 24:7-14

Astúa D (2010) Cranial sexual dimorphism in New World marsupials and a test of Rensch's rule in Didelphidae. J Mammal 91:1011-1024

Astúa D (2015) Morphometrics of the largest New World marsupials, opossums of the genus *Didelphis* Didelphimorphia, Didelphidae. Oecol Aust 19:117-142

Astúa de Moraes D, Hingst-Zaher E, Marcus LF, Cerqueira R (2000) A geometric morphometric analysis of cranial and mandibular shape variation in didelphid marsupials. Hystrix 11:115-130

Begg CM, Begg KS, Du Toit JT, Mills MGL (2003) Sexual and seasonal variation in the diet and foraging behaviour of a sexually dimorphic carnivore, the honey badger (*Mellivora capensis*). J Zool 260:301-316

Belk MC, Houston DD (2002) Bergmann's Rule in ectotherms: A test using freshwater fishes. Am Nat 160:803-808

Bergmann C (1847) Ueber die Verhältnisse der Wärmeökonomie der Thiere zu ihrer Grösse. Gottinger Studien, 3:595-708

Birks JDS, Dunstone N (1985) Sex- related differences in the diet of the mink *Mustela vison*. Ecography 8:245-252

Borcard D, Gillet F, Legendre P (2011) Numerical Ecology with R. Springer, New York

Bubadué JM, Cáceres NC, Carvalho RS, Meloro C (2016) Ecogeographical variation in skull shape of South American canids: abiotic or biotic processes? Evol Biol 43:145-149

Cáceres N (2002) Food habits and seed dispersal by the white-eared opossum, *Didelphis albiventris*, in southern Brazil. Stud Neotrop Fauna E 37:97-104

Cáceres NC (2003) Use of the space by the opossum *Didelphis aurita* Wied-Newied Mammalia, Marsupialia in a mixed forest fragment of southern Brazil. Rev Bras Zool 20:315-322

Cáceres NC, Machado AF (2013) Spatial, dietary and temporal niche dimensions in ecological segregation of two sympatric, congeneric marsupial species. Open Ecol J 6:10-23

Cáceres N, Meloro C, Carotenuto F, Passaro F, Sponchiado J, Melo GL, Raia P. (2014) Ecogeographical variation in skull shape of capuchin monkeys. J Biogeogr 41:501-512

Cáceres NC, Monteiro-Filho ELA (2001) Food habits, home range and activity of *Didelphis aurita* (Mammalia, Marsupialia) in a forest fragment of Southern Brazil. Stud Neotrop Fauna E 36:85-92

Cáceres NC, Weber MM, Melo GL, Meloro C, Sponchiado J, Carvalho RS, Bubadué JM (2016) Which factors determine spatial segregation in the South American opossums *Didelphis aurita* and *D. albiventris*? An ecological niche modelling and geometric morphometrics approach. PLoS One 11:e0157723

Cantor M, Ferreira AL, Silva WR, Setz EZF (2010) Potential seed dispersal by *Didelphis albiventris* Marsupialia, Didelphidae in highly disturbed environment. Biota Neotrop 10:45-51

Cardini A, Jansson AU, Elton S (2007) Ecomorphology of vervet monkeys: a geometric morphometric approach to the study of clinal variation. J Biogeogr 34:1663-1678

Cardini A (2014) Missing the third dimension in geometric morphometrics: how to assess if 2D images really are a good proxy for 3D structures? Hystrix 25:73-81

Cardini A (2016) Lost in the other half: improving accuracy in geometric morphometric analyses of one side of bilaterally symmetric structures. Syst Biol 65:1096-1106

Caumul R, Polly PD (2005) Phylogenetic and environmental components of morphological variation: skull, mandible, and molar shape in marmots (Marmota, Rodentia). Evolution 59: 2460-2472

Cardini A, Polly PD (2013) Larger mammals have longer faces because of size-related constraints on skull form. Nat Commun 4: 2458

Ceotto P, Finotti R, Santori R, Cerqueira R (2009) Diet variation of the marsupials *Didelphis aurita* and *Philander frenatus* (Didelphimorphia, Didelphidae) in a rural area of Rio de Janeiro state, Brazil. Mastozool Neotrop 16:49-58

Colles A, Liow LH, Prinzing A (2009) Are specialists at risk under environmental change? Neoecological, paleoecological and phylogenetic approaches. Ecol Lett 12:849-63

Costa LP, Patton JL (2006) Diversidade e limites geográficos e sistemáticos de marsupiais brasileiros. In: Cáceres NC, Monteiro-Filho ELA (eds) Os Marsupiais do Brasil: Biologia, Ecologia e Evolução. Editora UFMS, Campo Grande, pp 321-341

Cozzuol MA, Goin F, de Los Reyes M, Ranzi A (2006) The oldest species of *Didelphis* (Mammalia, Marsupialia, Didelphidae), from the late Miocene of Amazonia. J Mammal 87:663-667

Damasceno EM, Astúa D (2016) Geographic variation in cranial morphology of the Water Opossum *Chironectes minimus* Didelphimorphia, Didelphidae. Mammal Biol 81:380-392

Damasceno EM, Hingst-Zaher E, Astúa D (2013) Bite force and encephalization in the Canidae Mammalia: Carnivora. J Zool 290:246-254

Dias CAR, Perini FA (2018) Biogeography and early emergence of the genus *Didelphis* (Didelphimorphia, Mammalia). Zool Scr 2018:1-10

Diniz-Filho JAF, Bini LM, Hawkins BA (2003) Spatial autocorrelation and red herrings in geographical ecology. Global Ecol Biogeogr 12:53-64

Dos Reis SF, Duarte LC, Monteiro LR, Zuben FJV (2002) Geographic variation in cranial morphology in *Thrichomys apereoides* Rodentia: Echimyidae: II. Geographic units, morphological discontinuities, and sampling gaps. J Mammal 83:345-353

Dray S, Legendre P, Blanchet FG (2007) Packfor: forward selection with permutation. R package version 0.0-9. Available at: http://r-forge.r-project.org/R/group_id=195

Dray S, Legendre P, Peres-Neto PR (2006) Spatial modelling: a comprehensive framework for Principal Coordinate Analysis of Neighbour Matrices PCNM. Ecol Model 196:483-493

Dryden IL, Mardia KV (1998) Statistical Shape Analysis. John Wiley and Sons, New York

Fleming TH, Breitwisch R, Whitesides GH (1987) Patterns of tropical vertebrate frugivore diversity. Annu Rev Ecol Syst 18:91-109

Gardner A (2007) Mammals of South America, Vol. 1. Marsupials, Xenarthrans, Shrews, and Bats. University of Chicago Press, Chicago

Gohli J, Voje KL (2016) An interspecific assessment of Bergmann's rule in 22 mammalian families. Evol Biol 16:222

Hendges CD, Bubadué JM, Cáceres NC (2016) Environment and space as drivers of variation in skull shape in two widely distributed South American Tayassuidae, *Pecari tajacu* and *Tayassu pecari* Mammalia: Cetartiodactyla. Biol J Linnean Soc 119:785-798

Hendges CD, Patterson BD, Cáceres NC, Gasparini GM, Ross CF (2019) Skull shape and the demands of feeding: a biomechanical study of peccaries (Mammalia, Cetartiodactyla). J Mammal 100:475-486

Hijmans RJ, Cameron SE, Parra JL, Jones PG, Jarvis A (2005) Very high-resolution interpolated climate surfaces for global land areas. Int J Climatol 25:1965-1978

Hurlbert SH (1984) Pseudoreplication and the design of ecological field experiments. Ecol Monogr 54:187-211

Julien-Laferrière D, Atramentowicz M (1990) Feeding and reproduction of three didelphid marsupials in two Neotropical forests (French Guiana). Biotropica 22:404-415.

Kelley DB (1988. Sexually dimorphic behaviors. Annu Rev Neurosci 11:225-251

Klingenberg CP (2011) MorphoJ: an integrated software package for geometric morphometrics. Mol Ecol Resour 11:353-357

Koyabu D,Werneburg I, Morimoto N, Zollikofer CPE, Forasiepi AM, Endo H, Kimura J, Ohdachi SD, Son NT, Sánchez-Villagra MR (2014) Mammalian skull heterochrony reveals modular evolution and a link between cranial development and brain size. Nat Commun 5:3625

Maestri R, Luza AL, Barros LD, Hartz SM, Ferrari A, Freitas TRO, Duarte LDS(2016) Geographical variation of body size in sigmodontine rodents depends on both environment and phylogenetic composition of communities. J Biogeogr 43:1192-1202

Maestri R, Monteiro LR, Fornel R, de Freitas TR, Patterson BD (2018) Geometric morphometrics meets metacommunity ecology: environment and lineage distribution affects spatial variation in shape. Ecography 41: 90-100

Magnus LZ, Machado RF, Cáceres NC (2017) Comparative ecogeographical variation in skull size and shape of two species of woolly opossums genus *Caluromys*. Zool Anz 267:139-150

Magnus LZ, Machado RF, Cáceres NC (2018a) The environment is a major driver of shape and size variation in widespread extant xenarthrans. Mammal Biol 89: 52-61

Magnus LZ, Machado RF, Cáceres NC (2018b) Ecogeography of South-American Rodentia and Lagomorpha (Mammalia, Glires): roles of size, environment, and geography on skull shape. Zool Anz 277:33-41

McLean ML, McCay TS, Lovallo MJ (2005) Influence of age, sex and time of year on diet of the bobcat (*Lynx rufus*) in Pennsylvania. Am Mid Nat, 153(2):450-453

Medina AI, Martí DA, Bidau CJ (2007) Subterranean rodents of the genus *Ctenomys* (Caviomorpha, Ctenomyidae) follow the converse to Bergmann's rule. J Biogeogr 34:1439-1454

Meiri S, Yom-Tov Y, Geffen E (2007) What determines conformity to Bergmann's rule? Glob Ecol Biogeogr 16:788-794

Meloro C, Cáceres N, Carotenuto F, Passaro F, Sponchiado J, Melo GL, Raia P (2014a) Ecogeographical variation in skull morphometry of howler monkeys Primates: Atelidae. Zool Anz 253:345-359

Meloro C, Cáceres N, Carotenuto F, Sponchiado J, Melo GL, Passaro F, Raia F (2014b) In and out the Amazonia: evolutionary ecomorphology in howler and capuchin monkeys. Evol Biol 41:38-51

Meloro C, Raia P, Piras P, Barbera C, O'Higgins P (2008) The shape of the mandibular corpus in large fissiped carnivores: allometry, function and phylogeny. Zool J Linnean Soc 154:832-845Mendel SM, Vieira MV, Cerqueira R (2008) Precipitation, litterfall, and the dynamics of density and biomass in the black-eared opossum, *Didelphis aurita.* J Mammal 89:159-167

Monteiro LR, Duarte LC, dos Reis SF (2003) Environmental correlates of geographical variation in skull and mandible shape of the punaré rat *Thrichomys apereoides* (Rodentia: Echimyidae). J Zool 261:47-57

Oksanen J, Kindt R, Legendre P, O'Hara RB (2012) Vegan: community ecology package. R package version 2.0-5. Available at: http://cran.rproject.org/web/packages/vegan/index.html

Pigliucci M, Murren CJ, Schlichting CD (2006) Phenotypic plasticity and evolution by genetic assimilation. J Exp Biol 209:2362-2367

Piras P, Salvi D, Ferrara G, Maiorino L, Delfino M, Pedde L, Kotsakis T (2011) The role of post-natal ontogeny in the evolution of phenotypic diversity in *Podarcis* lizards. J Evol Biol 24: 2405-2720

Post E, Langvatn R, Forchhammer MC, Stenseth NC (1999) Environmental variation shapes sexual dimorphism in red deer. Proc Natl Acad Sci USA 96:4467-4471

R Core Team 2016. R: a language and environment for statistical computing. R Foundation for Statistical Computing. Vienna, Austria. Available at: https://www.R-project.org/

Rensch B (1950) Die Abhängigkeit der relativen Sexualdifferenz von der Körpergrösse. Bonn Zool 1:58-69

Rohlf FJ (2015) The tps series of software. Hystrix 26:9-12

Meloro C et al. (2014a) Ecogeographical variation in skull morphometry of howler monkeys Primates: Atelidae. Zool Anz 253:345-359

Rossi RV, Carmignotto AP, Oliveira MVB, Miranda CL, Cherem JJ (2012) Diversidade e diagnose de espécies de marsupiais brasileiras. In: Cáceres NC (ed) Os marsupiais do Brasil: biologia, ecologia e conservação. Editora UFMS, Campo Grande, pp 23-74

Ryser J (1992) The mating system and male mating success of the Virginia opossum *Didelphis virginiana* in Florida. J Zool 228:127-139

Sansalone G, Colangelo P, Kotsakis T, Loy A, Castiglia R, Bannikova AA, Zemlemerova ED, Piras P (2018) influence of evolutionary allometry on rates of morphological evolution and disparity in strictly subterranean moles (Talpinae, Talpidae, Lipotyphla, Mammalia). J Mammal Evol 25:1-14

Sansalone G, Kotsakis T, Piras P (2015) *Talpa fossilis* or *Talpa europaea*? Using geometric morphometrics and allometric trajectories of humeral moles remains from Hungary to answer a taxonomic debate. Palaeontol Electron 18:1-17

Schiaffini MI (2016) A test of the Resource's and Bergmann's rules in a widely distributed small carnivore from southern South America, *Conepatus chinga* (Molina, 1782) (Carnivora: Mephitidae). Mammal Biol 81: 73-81

Schiaffini MI, Segura V, Prevosti FJ (2019) Geographic variation in skull shape and size of the Pampas fox *Lycalopex gymnocercus* (Carnivora: Canidae) in Argentina. Mammal Biol 97:50-58

Silva AR, Forneck ED, Bordignon SAL, Cademartori CV (2014) Diet of *Didelphis albiventris* Lund, 1840 Didelphimorphia, Didelphidae in two periurban areas in southern Brazil. Acta Sci 36:241-247

Stumpp R, Fuzessy L, Paglia AP (2018) Environment drivers acting on rodent rapid morphological change. J Mammal Evol 25(1): 131-140

Sunquist ME, Austad SN, Sunquist F (1987) Movement patterns and home range in the common opossum (*Didelphis marsupialis*). J Mammal 68:173-176

Sunquist ME, Eisenberg JF (1993) Reproductive strategies of female *Didelphis*. Bull Fla Mus Nat Hist Biol Sci 36:109-140Ungar PS (2010) Mammal Teeth: Origin, Evolution, and Diversity. Johns Hopkins University Press, Baltimore

Van Valkenburgh BV (1991) Iterative evolution of hypercarnivory in canids Mammalia: Carnivora: evolutionary interactions among sympatric predators. Paleobiology 17:340-362

Zelditch ML, Swiderski DL, Sheets HD 2012. Geometric Morphometrics for Biologists: A Primer. Academic Press, Cambridge

Figure Legends

Figure 1. Scaled map of South America with the IUCN distributional range of the three species used in this study and zoomed images of the three distributions with the collection points for out dataset. *Didelphis marsupialis* represented by square symbols, *D. aurita* by triangles and *D. albiventris* by circles. Filled and smaller symbols are representing male samples and large and unfilled symbols are females.

Figure 2. Disposition of 25 landmarks on both sides of the skull of *Didelphis albiventris* (MZUSP 17381). 1 = midpoint of central incisors; 2 = posterior-most point of lateral incisor alveolus; 3–5 = canine area; 5–7 = pre-molar series length; 6–8 = first molar area; 9–11 = second molar area; 12–14 = third molar area; 15–17 = fourth molar area; 18–21 = temporal muscle insertion area; 22 = most posterior tip of the palatine; 23–25 = occipital condyle area.

Figure 3. Scatter plot of PC1 vs PC2. Transformation grids visualize shape deformations relative to the mean at the positive and negative extremes of the Principal Component axes. Every species is labelled according to different color and symbol within minimum convex hull superimposed. F is for females and M is for males.

Figure 4. Slope comparison plot showing the predicted shape versus the size (Ln Centroid Size) of Didelphis skull. Deformation plots show relative shape changes from the smallest to the largest specimen for each species and sexes. Every species is labelled according to different color and symbol. Find the prediction percentage and P value for each species bellow its prediction line.

Figure 5. Schematic depiction of the factors analyzed in partition variation to illustrate their individual contribution and their interaction components in the variance of skull a) size and b) shape; and skull c) size and d) shape sexual dimorphism. Values < 0 not shown.

Figure 6. Plots showing the relationship between sexual a) size and b) shape dimorphism and climate of *Didelphis* skull. Every species is labelled according to different color and symbol. Symbols increase with sexual dimorphism values.

Figure 7. Plots with the clinal variation of size and shape of *D. albiventris* and *D. marsupialis*. Size plots in a) *D. albiventris* and b) *D. marsupialis*. Shape Partial Least Squares plots with associated deformation grids from the most negative to the most positive PLS scores in c) *D. albiventris* and d) *D. marsupialis*. Open symbols are females, filled ones are males.

Tables

Table 1. Number of specimens, localities and grids separated by species and sexes of *Didelphis*. FS = Female Specimens; MS = Male Specimens; FL = Female Localites; ML = Male Localities; SD = Sexual dimorphism

	#FS	#MS	#Specimens	#FL	#ML	#Localities	#SD Grids
D. albiventris	86	88	174	50	45	95	21
D. aurita	68	91	159	36	46	82	16
D. marsupialis	43	37	80	28	22	50	13
Total	197	216	413	114	113	227	50

Table 2. Pairwise slope comparisons between species and sexes of *Didelphis*. Upper diagonal is either slope length contrast values or angles between slope vectors. Lower diagonals are P values for each comparison.

Pairwise differences in slope length contrast						
	D. albiventris Female	*D. albiventris* Male	*D. aurita* Female	*D. aurita* Male	*D. marsupialis* Female	*D. marsupiais* Male
D. albiventris Female		0.010	0.005	0.225	0.062	0.078
D. albiventris Male	0.778		0.005	0.215	0.071	0.088
D. aurita Female	0.943	0.951		0.220	0.067	0.084
D. aurita Male	**0.000**	**0.000**	**0.009**		0.287	0.303
D. marsupialis Female	0.191	0.121	0.393	**0.000**		0.017
D. marsupialis Male	0.175	0.123	0.332	**0.000**	0.803	
Pairwise differences in angles between slope vectors						
	D. albiventris Female	*D. albiventris* Male	*D. aurita* Female	*D. aurita* Male	*D. marsupialis* Female	*D. marsupialis* Male
D. albiventris Female		13.46923	29.47204	30.70127	40.98486	42.87029
D. albiventris Male	0.273		34.27065	23.2719	37.52358	37.07128
D. aurita Female	0.3353	0.203		42.09161	37.26995	38.66385
D. aurita Male	**0.0329**	0.1392	0.1403		29.53142	32.97297
D. marsupialis Female	**0.0018**	**0.0034**	0.2001	0.1118		30.32558
D. marsupialis Male	**0.0199**	**0.0379**	0.2471	0.1478	0.1832	

Table 3. Results from pairwise comparisons, between species and sexes of *Didelphis*, of standardized shapes at large and small sizes for the allometric convergency test. PDL = Procrustes distances between means at large sizes; PDS = Procrustes distances between means at small sizes; D. alb = *D. albiventris*, *D. aur* = *D. aurita*, *D. mar* = *D. marsupialis.* F = Females; M = Males. Significant results in bold ($P < 0.05$).

Comparative Pairs	PDL	P value	PDS	P value
D. alb F-*D. alb* M	0.035	**0.004**	0.025	0.065
D. alb F-*D. aur* F	0.031	**0.018**	0.028	**0.003**
D. alb F-*D. aur* M	0.030	**0.004**	0.035	**0.004**
D. alb F-*D. mar* F	0.027	**0.015**	0.027	**0.021**
D. alb F-*D. mar* M	0.040	**0.000**	0.036	0.088
D. alb M-*D. aur* F	0.055	**0.000**	0.047	**0.000**
D. alb M-*D. aur* M	0.025	**0.001**	0.023	0.135
D. alb M-*D. mar* F	0.040	**0.000**	0.042	**0.001**
D. alb M-*D. mar* M	0.034	**0.000**	0.030	0.124
D. aur F-*D. aur* M	0.039	**0.000**	0.044	**0.000**
D. aur F-*D. mar* F	0.021	**0.043**	0.013	0.229
D. aur F-*D. mar* M	0.045	**0.000**	0.038	**0.002**
D. aur M-*D. mar* F	0.025	**0.000**	0.038	**0.002**
D. aur M-*D. mar* M	0.015	**0.031**	0.015	0.477
D. mar F-*D. mar* M	0.024	**0.002**	0.024	0.161

Supplementary Data

Supplementary Data SD1. List of 413 *Didelphis* specimens used for morphometric analyses, with data on species, museum, record number from museum, sex, geographical coordinates (latitude and longitude in decimal degrees), centroid size (CS), Natural Logarithms of Centroid Size (LnCS), Procrustes Coordinates (C#). Averaged values are bellow each correspondent set of specimens that were added to that average. MCNFZB: Museu de Ciências Naturais da Fundação Zoobotânica do Rio Grande do Sul, MN: Museu Nacional (PI and CA is for specimens in the museum with no record aside for the collector number), MPEG: Museu Paraense Emílio Goeldi, MHNCI = Museu de História Natural Capão da Imbuia, UFSC: Coleção Científica do Laboratório de Mamíferos Aquáticos da UFSC, MACN: Museo Argentino de Ciencias Naturales ‘‘Bernardino Rivadavia’’, MZUSP: Museu de Zoologia da Universidade de São Paulo.Supplementary Data SD2. Sexual size and shape dimorphism data

Supplementary Data SD2. Sexual size (SSD) and shape dimorphism (SShD) data separated by species. Central coordinates for each grid are given in decimal degrees. Mean male size (MSize) and female size (FSize) for each grid was calculated by averaging the specimens present in each grid.

Figure1

Click here to access/download;Figure;Fig1.tif

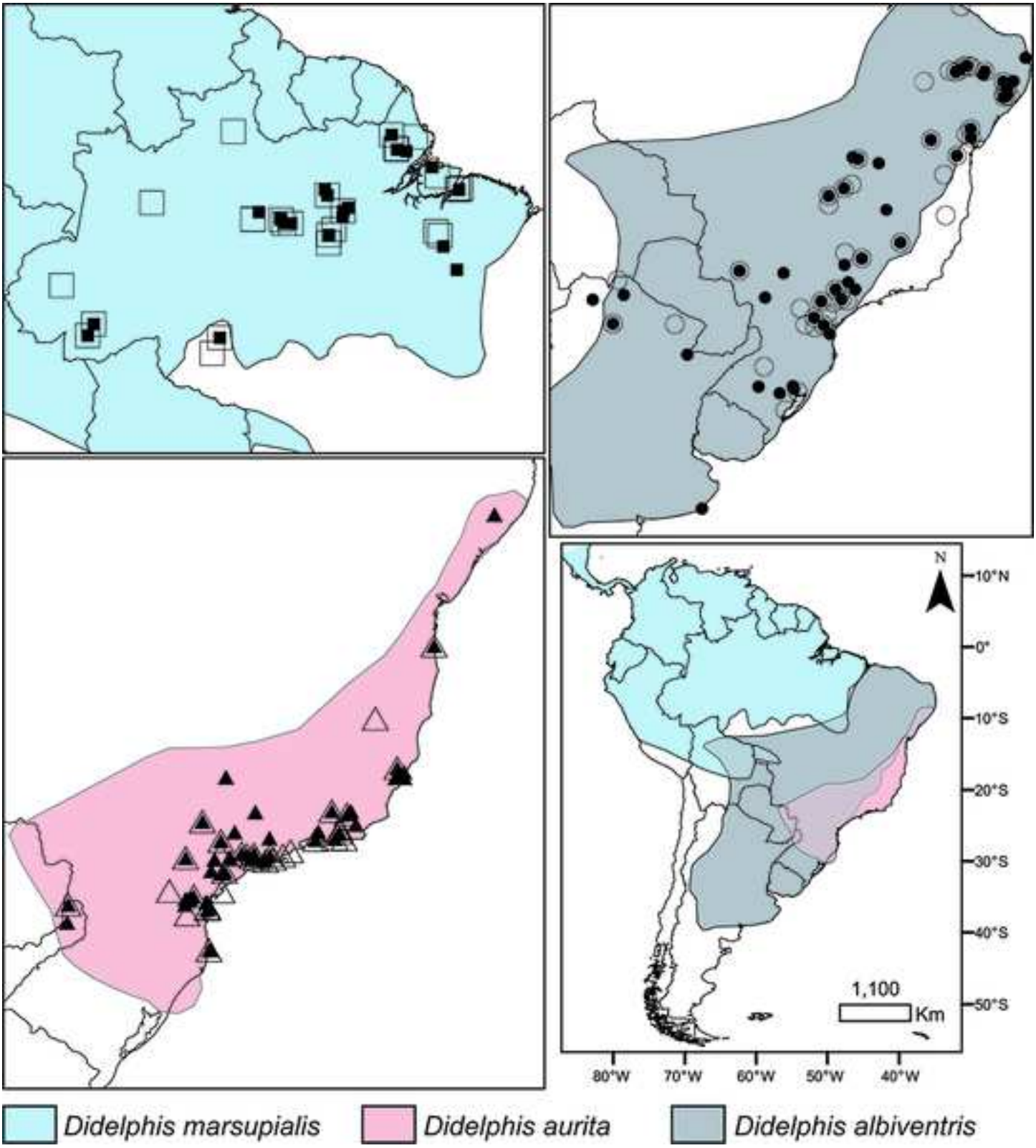

Figure2

Click here to access/download;Figure;Fig2.tif

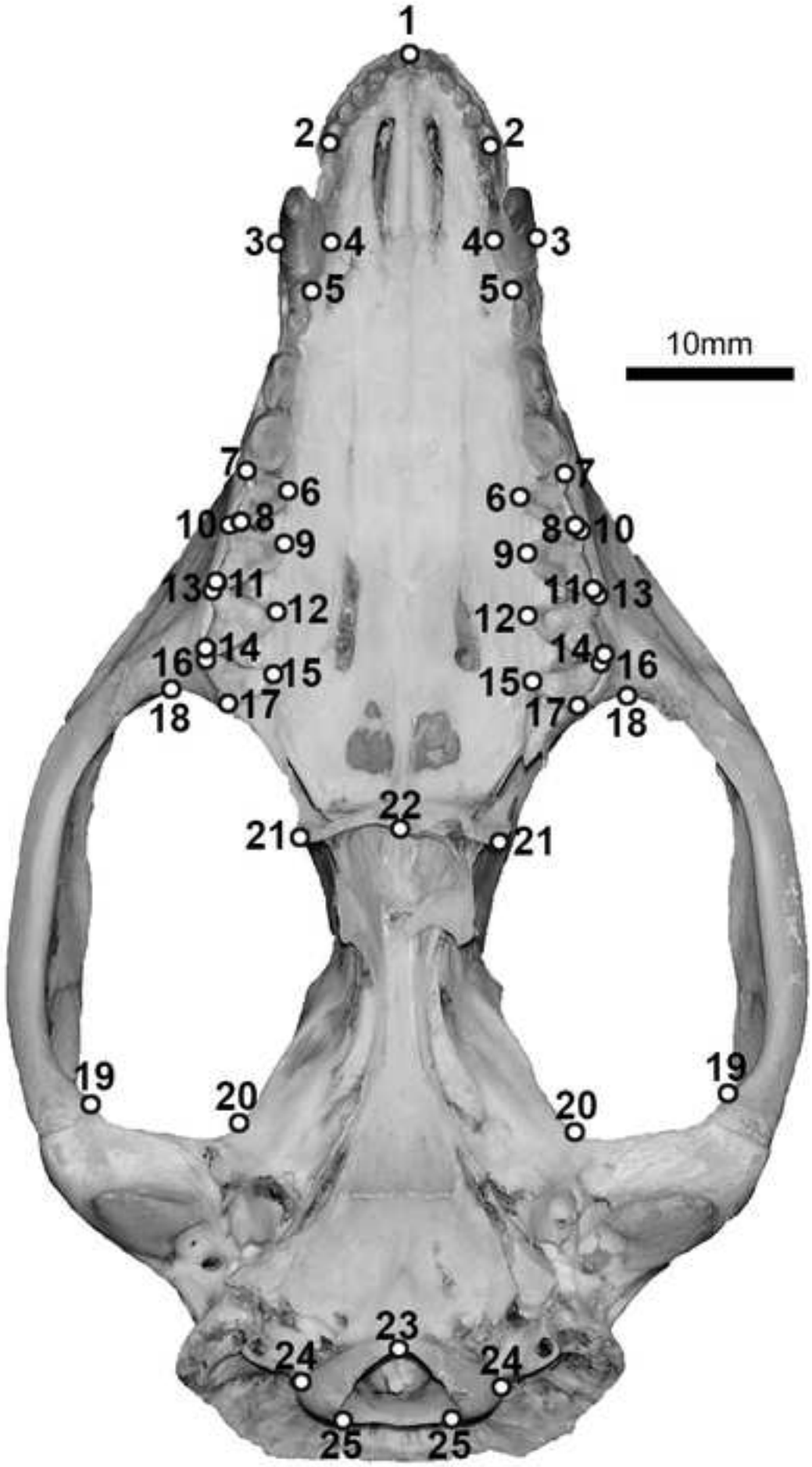

Figure3

Click here to access/download;Figure;Fig3.tif

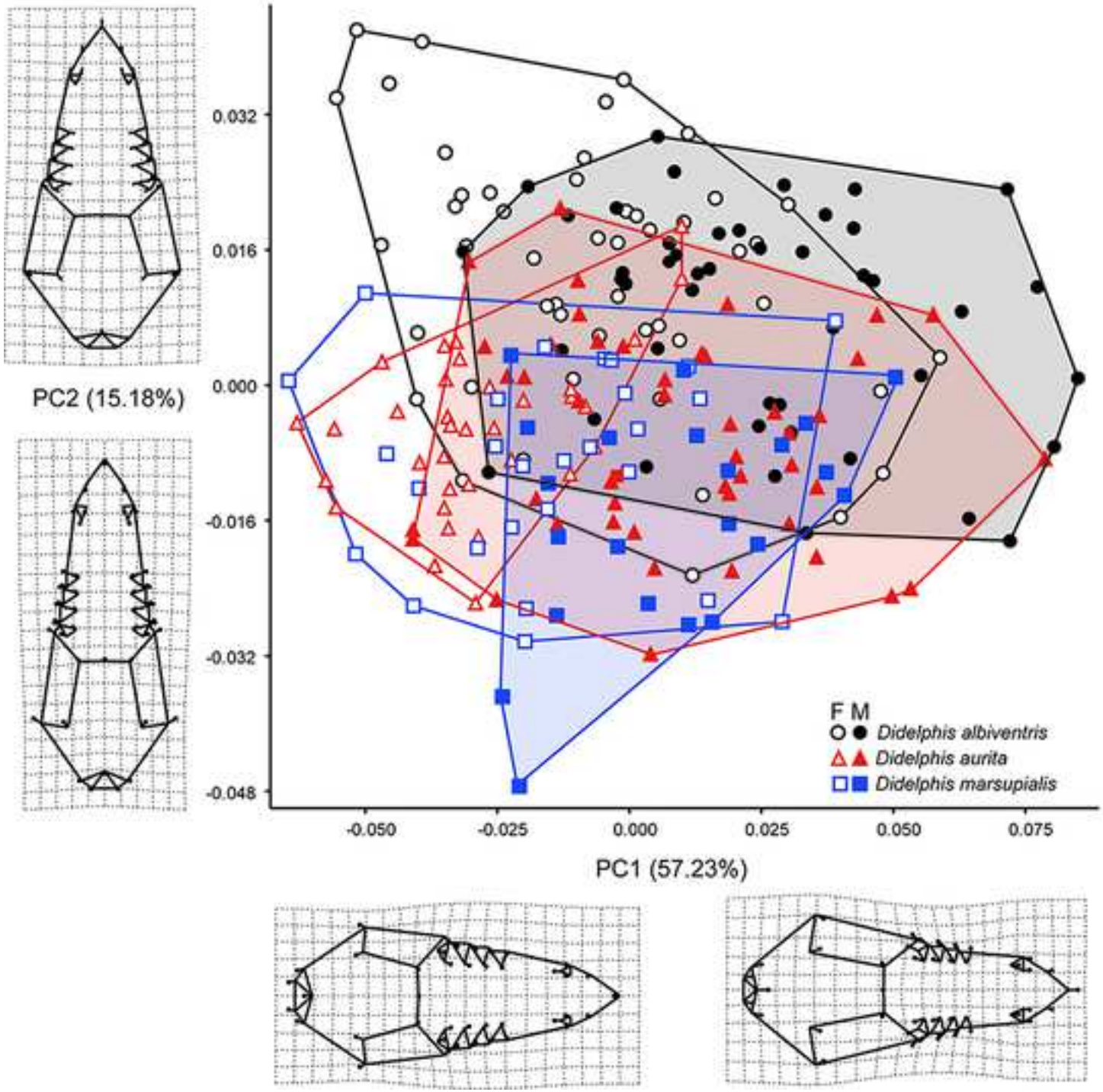

Figure4

Click here to access/download;Figure;Fig4.tif

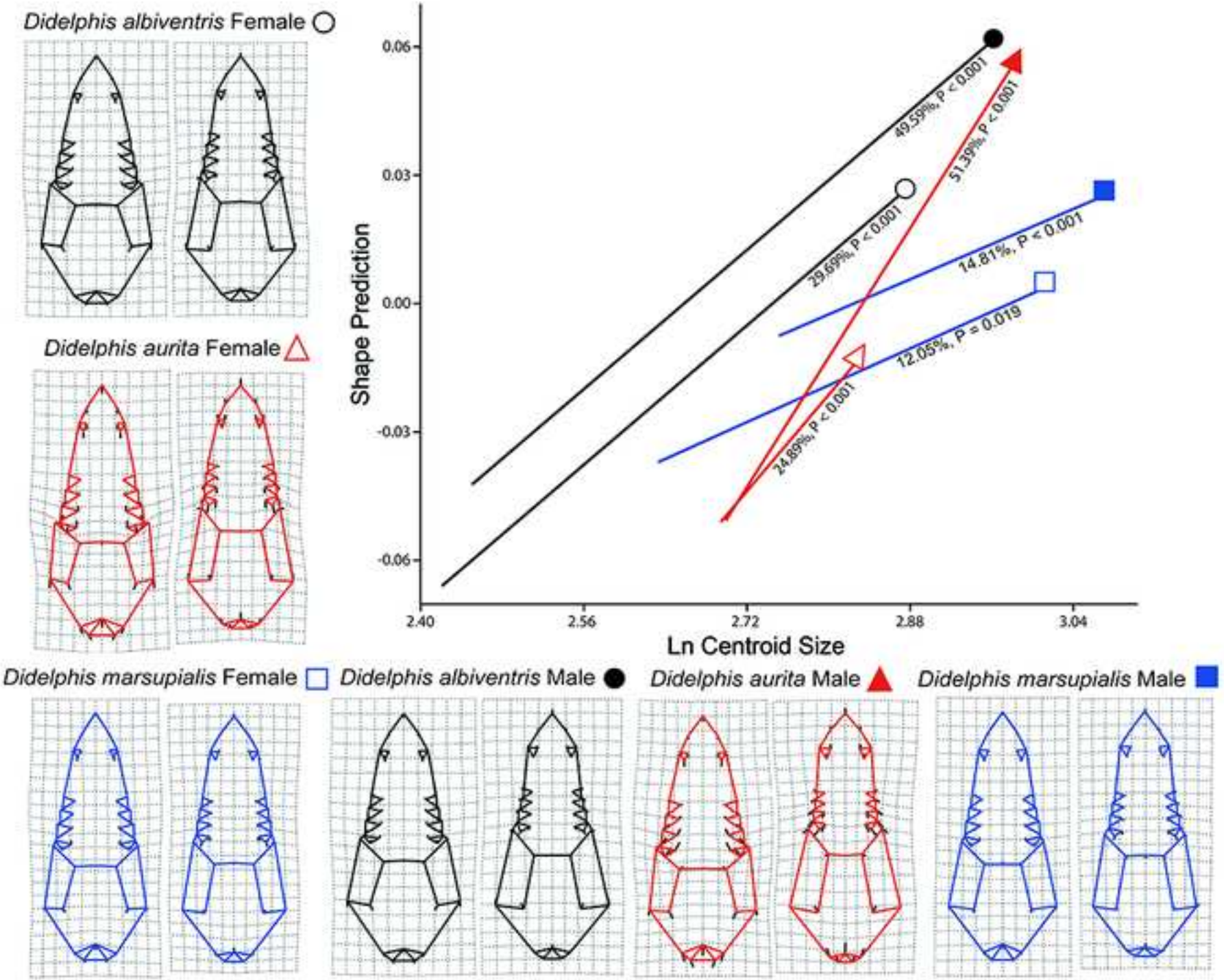

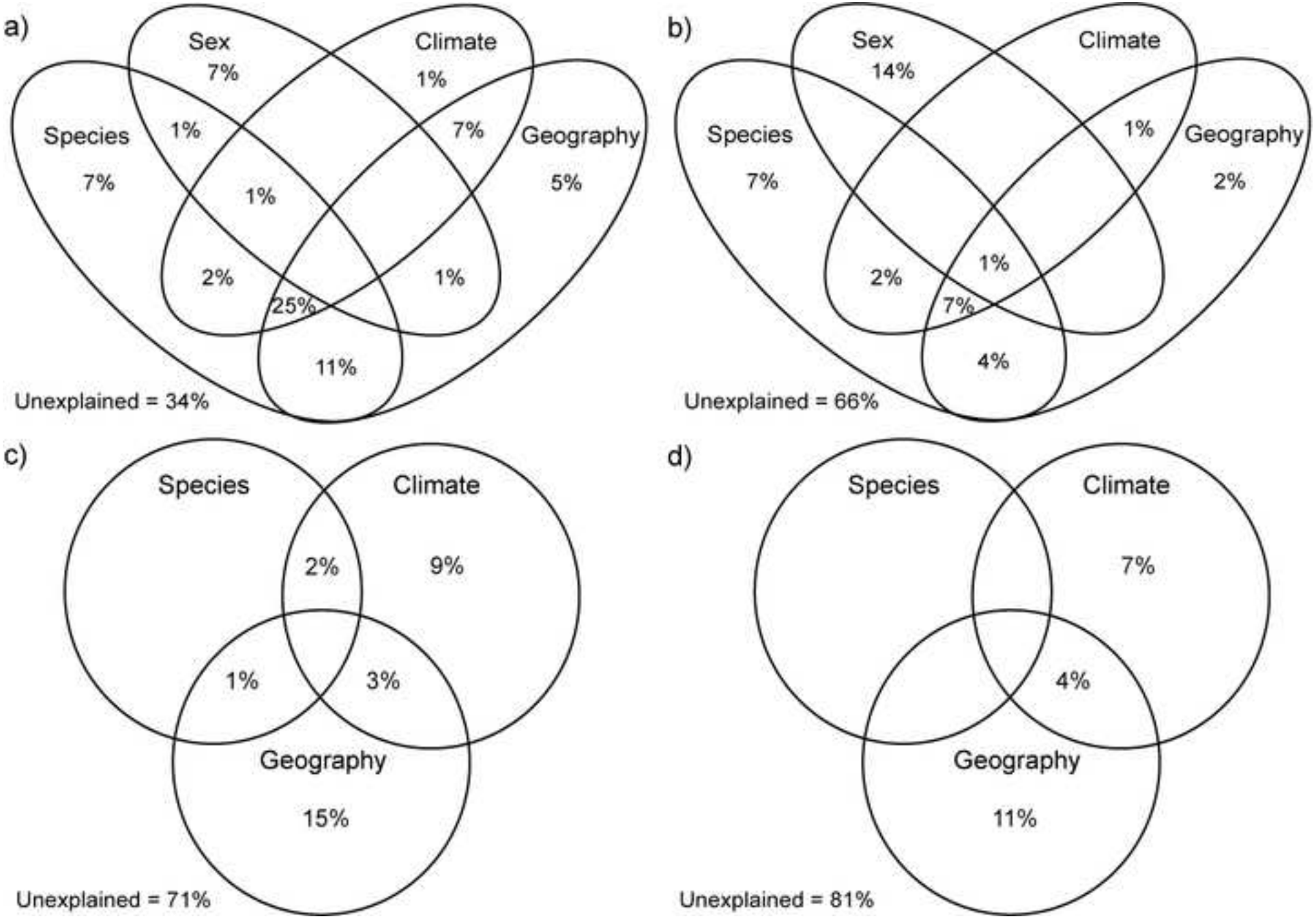

Figure6

Click here to access/download;Figure;Fig6.tif

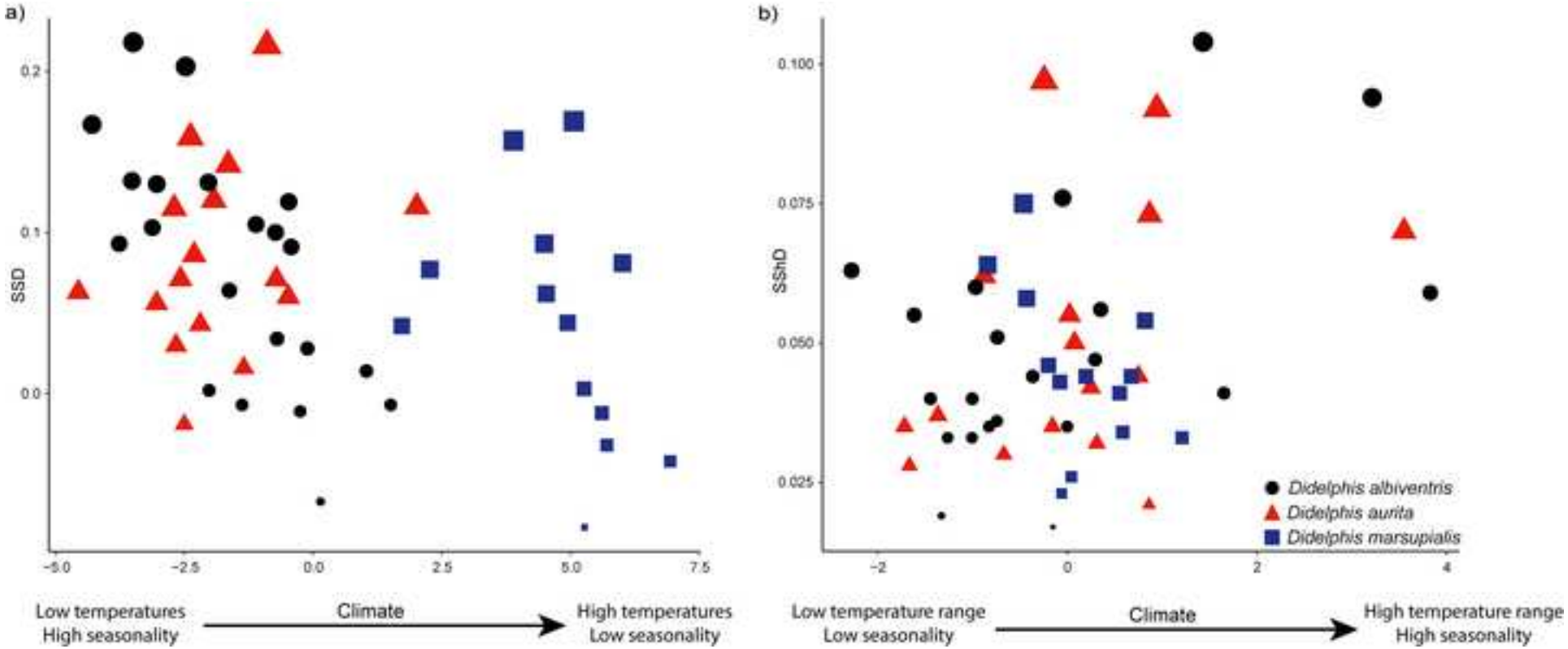

Figure7

Click here to access/download;Figure;Fig.7.tif

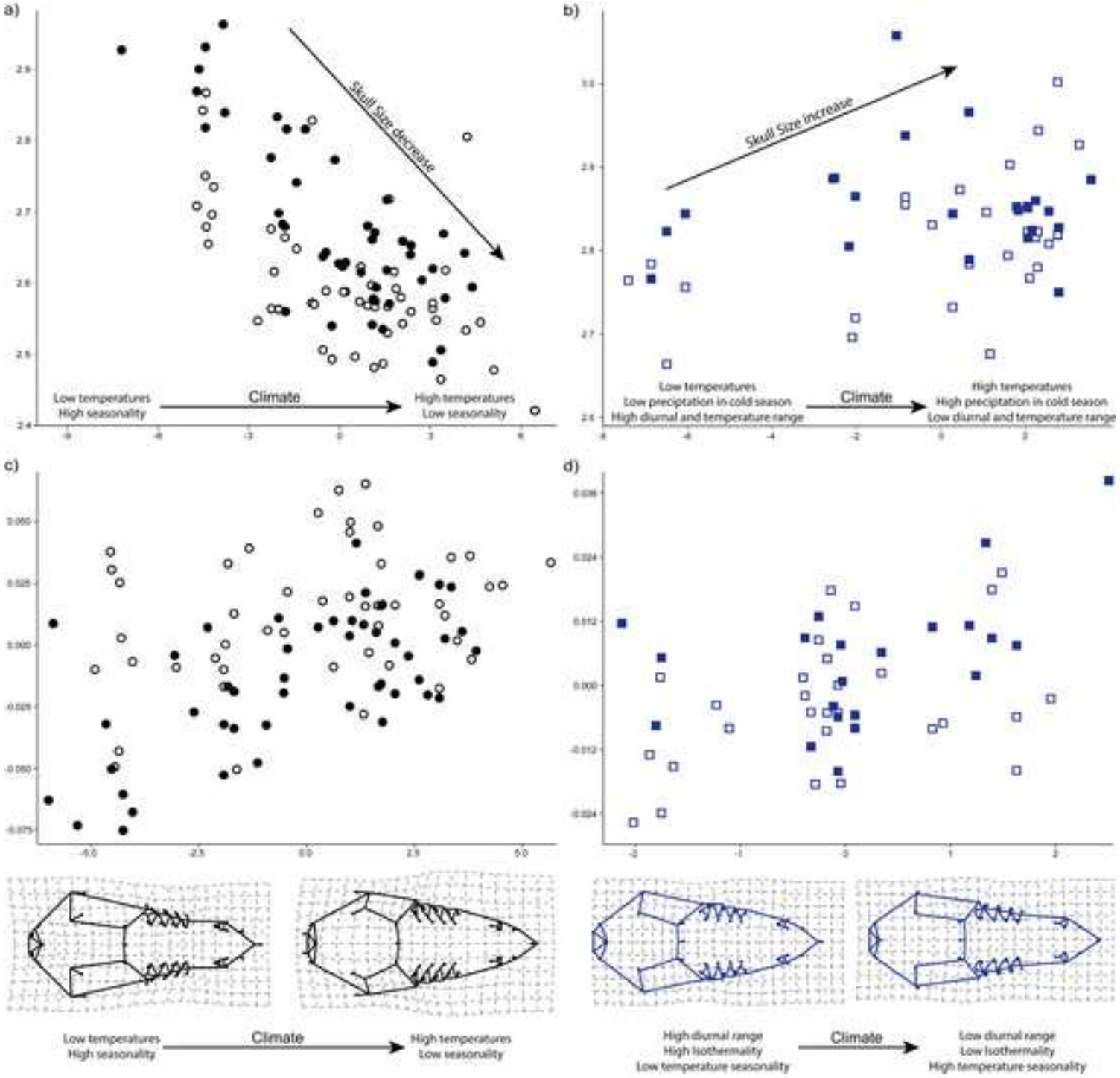

Click here to access/download

Supplemental Material

SD1.xlsx

Click here to access/download

Supplemental Material

SD2.docx